Fire Safety Journal 71 (2015) 340–352

Contents lists available at ScienceDirect

Fire Safety Journal

journal homepage: www.elsevier.com/locate/firesaf

# An experimental investigation of mechanical properties of structural cast iron at elevated temperatures and after cooling down

C. Maraveas [a], Y.C. Wang [a,*], T. Swailes [a], G. Sotiriadis [b]

[a] School of Mechanical, Aerospace and Civil Engineering, University of Manchester, UK
[b] Applied Mechanics and Vibrations Lab, Department of Mechanical Engineering, University of Patras, Rio, Greece

ARTICLE INFO

*Article history:*
Received 17 June 2014
Received in revised form
24 November 2014
Accepted 30 November 2014

*Keywords:*
Mechanical properties
Cast iron
High temperatures
Stress strain temperature relationship
Thermal expansion
Residual strength

ABSTRACT

This paper presents the results of an extensive experimental investigation of the mechanical properties of structural cast iron at elevated temperatures and after cooling down to room temperature. A total of 135 tests were carried out. The specimens were subjected to tension (83 tests), compression (48 tests) or were heated for measurement of the thermal expansion (4 tests). The tests in tension include 35 steady-state tests up to 900 °C, 32 transient tests (5 °C/min and 20 °C/min heating rates, applied stress from 20% to 80% of 0.2% proof stress) and 16 tests after cooling down (heated up to 800 °C and cooled down with two different methods: quenching and air flow cooling). 32 steady-state tests (up to 900 °C) and 16 transient tests (5 °C/min and 20 °C/min heating rates, applied stress from 50% to 120% of 0.2% proof stress) were carried out for specimens in compression. The paper evaluates and proposes elevated temperatures material models.



## 1. Introduction

From the middle of the 18th until the beginning of the 20th century [1], cast iron elements were commonly encountered in the structural framing of buildings in Great Britain, United States and Central and Northern Europe [2–9]. However, since cast iron is no longer a mainstream construction material, there is a lack of extensive research on this type of construction. Furthermore, of the research investigations conducted on cast iron structures, most have been focused on their ambient temperature behavior [10–14]. Although there have been some efforts of evaluating the behavior of cast iron structural members in fire conditions, such studies have either been based on early fire tests or largely qualitative observations of their response in fire incidents [15–23]. There was a general lack of rigor when evaluating fire performance of cast iron structures even when dealing with rehabilitation of the fire exposed cast iron construction [22,23]. A main reason for the limited treatment of this subject is the lack of reliable data regarding the mechanical behavior of cast iron at elevated temperatures and after cooling down. The detailed survey of literature by the present authors [24] has revealed that there is a good number of historical sources of data on various aspects of mechanical properties of cast iron at elevated temperatures [25–28]. However, there is a large scatter in results from these different sources. Also, these earlier references often lack detailed information on the experimental methodology as well as composition of the cast iron investigated. To enable accurate assessment of the fire resistance of cast iron structures and their residual structural performance after cooling down, it is clearly important that reliable mechanical property data is available. The follow-on sensitivity study by the present authors [29] has shown that the fire resistance of cast-iron structural members is particularly sensitive to the following mechanical properties: strength, thermal expansion and modulus of elasticity. Providing detailed experimental information on elevated temperature and residual mechanical properties of cast iron is the focus of this paper.

This paper presents the results of an extensive experimental program involving a total of 135 cast iron specimens subjected to elevated temperature effects. Both steady-state and transient heating conditions were applied. Since cast iron has different tensile and compressive properties, the specimens were tested in tension and compression. Furthermore, a total of 16 specimens were tested to measure their residual strengths after cooling down from high temperatures. Two different cooling methods were used, one natural cooling and one quenching with cold water. Based on the test results, mathematical expressions have been proposed for the mechanical property–temperature relationships.

* Corresponding author.
*E-mail address:* yong.wang@manchester.ac.uk (Y.C. Wang).

http://dx.doi.org/10.1016/j.firesaf.2014.11.026
0379-7112/

## 2. Testing arrangement

### 2.1. Test specimens

The test specimens were made from two cast iron columns with a circular hollow cross-section. These columns came from the Orangery at Tatton Park in Cheshire in the UK. 65 specimens with dimensions shown in Fig. 1a were made from the first column (material 1, Table 1) and were prepared for tensile testing according to EN ISO 6892-1: 2009 [30]. The grip part of the specimens tested at room temperature was made into three specimens for thermal expansion testing. From the other column (material 2, Table 1), 17 specimens (with dimensions shown in Fig. 1b) were prepared for tensile testing according to the same standard [30] and 49 specimens (with dimensions shown in Fig. 1c and d) were prepared for compression testing according to the ASTM E9-09 [31] and ASTM E209-00 [32] standards. The chemical compositions of the materials are presented in Table 1. Fig. 2 shows the typical microstructure of the test specimens, which clearly differs from that of a homogeneous material.

### 2.2. Testing device

The testing devices include a type 8802 INSTRON Universal Testing Machine of 250 kN maximum capacity, a type SC1706 short electric furnace with a maximum heating capability of 1400 °C, a spring-loaded type thermo-couple (placed on the specimen to measure the specimen temperature) and an Epsilon CP8830C (25 mm/ ± 20%) high temperature extensometer. Fig. 3 shows the experimental arrangement.

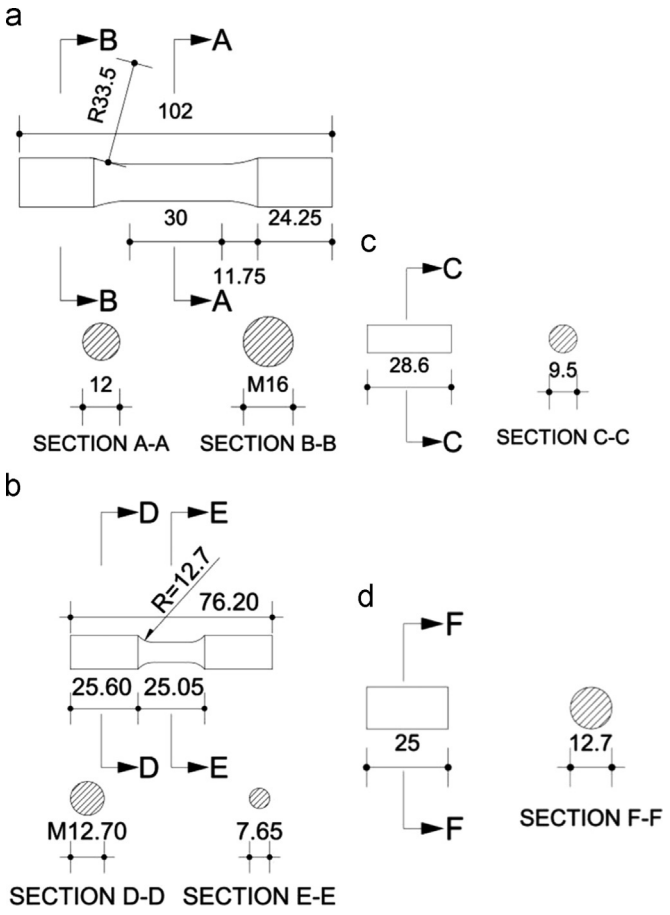


**Fig. 1.** Cast iron specimens for tensile and compressive tests (units in mm): (a) tensile specimen (material 1), (b) tensile specimen (material 2), (c) compressive specimen (material 2) and (d) thick compressive specimen (material 1).

### 2.3. Test procedure

The tests were categorized in eight groups (A–H) according to the heating method, the type of stress applied (tensile or compressive) and the testing condition (during heating or after cooling down). Table 2 provides details of the experimental program.

## 3. Tensile mechanical properties of cast iron at elevated temperatures

### 3.1. General

It is known [33] that cast iron does not exhibit a distinct yield stress point and that its stiffness in tension changes as the various flaws in its microstructure open [28,34]. For this reason, a clear definition of the mechanical properties (i.e. yield stress, fracture stress etc.) presented in this paper is given below. These are generally in accordance with Refs. [25,28,33] pertaining to the experimental investigation of the mechanical properties of cast iron.

In Fig. 4, a typical stress–strain diagram of cast iron in tension is presented. From this it can be observed that the initial tangent modulus, which is typically (in other materials) assumed to be equal to Young's modulus of elasticity, does not follow the stress–strain diagram, except for the region in which the strain has small values. For this reason, the tensile elastic modulus in this paper is assumed to be equal to the secant modulus of elasticity at 0.2% proof stress. The yield strength is defined, conventionally, as the 0.2% proof stress based on using the initial tangent modulus. The proportional limit does not have to be defined, because, practically, there is no linear region in the stress–strain diagram. The ultimate tensile strength $f_u$ is defined as the maximum stress in the diagram and the fracture stress $\sigma_f$ is the stress at the failure (breaking) point of the specimen. In general, $f_u/\sigma_f = 1$, but for temperatures higher than 500 °C this ratio reduces below unity ($f_u/\sigma_f < 1$).

The observed failure mode in all specimens was brittle, intergranular, without necking around the failure region (Fig. 5a). At temperatures exceeding 700 °C, the fracture surface was less flat (Fig. 5b), which is an indication of a moderately brittle fracture. Some of the specimens tested at 700 °C and 800 °C failed through multiple surfaces (Fig. 5c), which suggests that the increased elongation of the specimens in the high temperature region may have led to a different failure mechanism, most possibly as a result of opening of the flaws. Because necking of the specimens is not observed, i.e. the cross-section is not altered, the engineering stress is identical with the true stress. During these tests, the behavior of the material when near failure in tension was unstable, with the results from the duplicate specimens at the same temperature showing some inconsistence. The duplicate specimens were made from the opposite sides of the same cast iron column. A chemical analysis of these specimens showed a 0.05% difference in the carbon content, which may have contributed to the difference in results.

The specimens from Group E, which were intended for testing at 1000 °C, failed at 950–965 °C under a small prestress load of approximately 5 N (applied to stabilize the extensometer). The corresponding specimens in Group B displayed stable behavior at 1000 °C when the applied load was low. A possible explanation for this is the small diameter of the specimens in Group E.

**Table 1**
Chemical compositions of the cast iron test specimens

| Material | C (%) | Mn (%) | Si (%) | P (%) | S (%) | Ni (%) | Cr (%) | Mo (%) | Cu (%) |
|---|---|---|---|---|---|---|---|---|---|
| 1 | 2.90–2.95 | 0.36 | 1.41 | 0.65 | 0.21 | 0.02 | – | – | 0.02 |
| 2 | 3.075 | 0.488 | 1.37 | 0.595 | 0.14 | – | – | – | – |

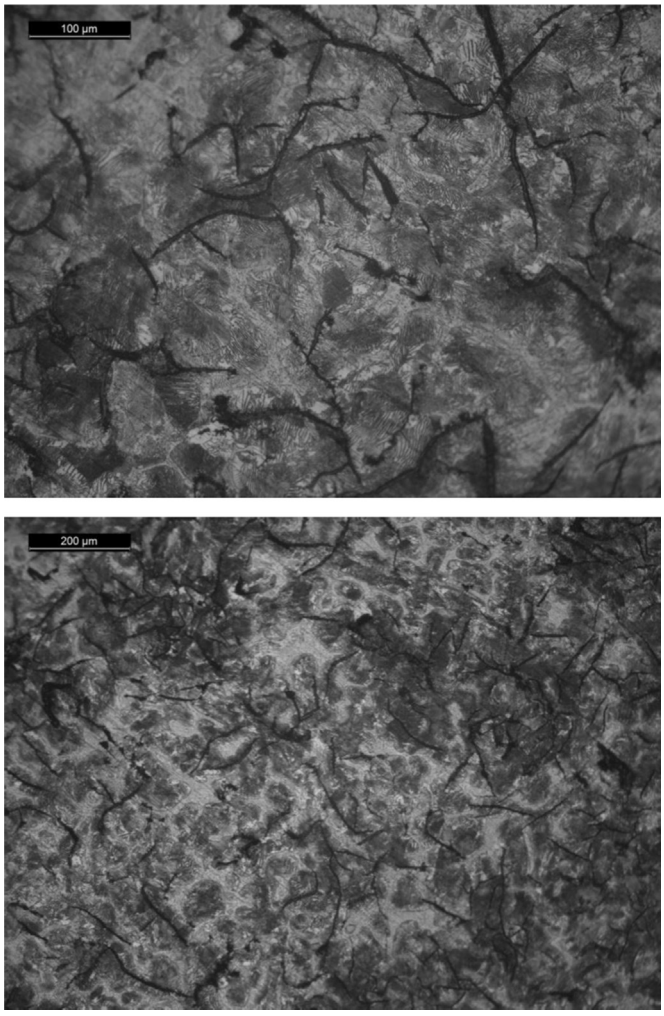


**Fig. 2.** Microstructure of cast iron test specimens (200× (upper), 100× (lower)).

### 3.2. Stress–strain curves in tension

Fig. 6 presents the recorded stress–strain curves from the steady state tests at different temperatures for group A and group E specimens. As can be seen, the stress–strain curves were not influenced up to temperatures of 400 °C and failure occurred at strains of about 0.5%. The mechanical response of Material 1 (Table 1) remained unaffected even at 500 °C (Fig. 6a and b), whereas Material 2 at 500 °C (Fig. 6c) failed at strain equal to 1.2%, accompanied by a minor decrease in strength. For temperatures above 500 °C, ductile behavior was observed with failure occurring at strains of 1.8% for 600 °C and at 4% for higher temperatures (with the exception of Fig. 6a, which shows an earlier failure for the corresponding specimen). It is worth noting that the stress–strain curves are nonlinear in the entire strain range.

Fig. 7 show the temperature–strain relationships from the transient state tests for group B specimens. From such curves, the transient stress–strain curves were obtained following the procedure of [35]. Fig. 8 shows typical comparison of stress–strain curves from the steady-state and transient state tests. The results show little difference between the steady state and the transient stress–strain diagrams, with the transient strengths being slightly higher than the steady state values.

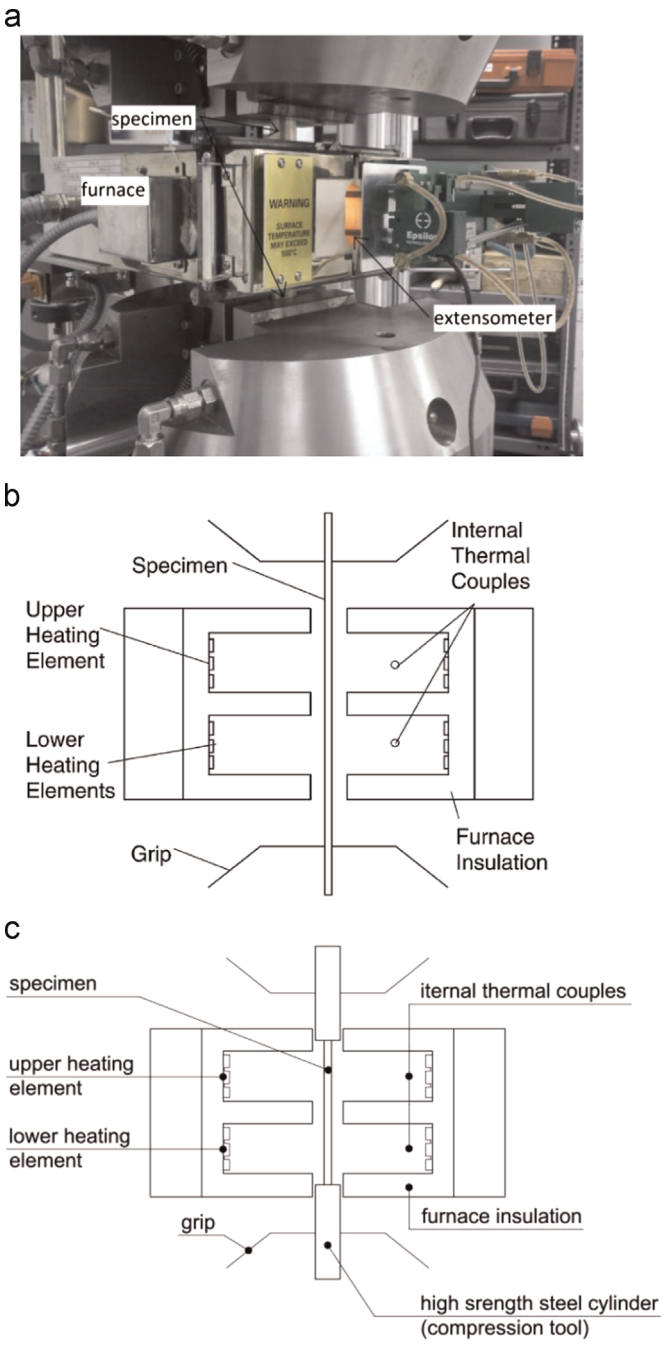


**Fig. 3.** (a) High-temperature tensile and compressive testing device, (b) general arrangement of the tensile tests and (c) general arrangement of the compression tests.

**Table 2**
Test program with details.

| Group no. | Specimen type (Fig. 1) | Material (Table 1) | Type of test | Heating method | Cooling method | Number of specimens | Test temperatures | Initial stress level | Heating rate | Strain rate |
|---|---|---|---|---|---|---|---|---|---|---|
| A | (a) | 1 | Tension | Steady state | – | 18 | 20 °C, 100–800 °C @100 °C interval | – | 5 °C/min | 0.5 mm/min |
| B | (a) | 1 | Tension | Transient | – | 32 | – | 10–80% @ interval of 10% of 0.2% proof stress (185 MPa) | 5 °C/min<br>20 °C/min | – |
| C | Cube 10 × 10 × 7 (mm) & (c) | 1 | Thermal expansion | – | – | 3+1 | 100–800 °C @100 °C | – | 10 °C/min | – |
| D-1 | (a) | 1 | Tension after cooling down | Steady state | Water quenching | 8 | 100–800 °C @100 °C | – | 5 °C/min | 0.5 mm/min |
| D-2 | (a) | 1 | Tension after cooling down | Steady state | Air flow | 8 | 100–800 °C @100 °C | – | 5 °C/min | 0.5 mm/min |
| E | (b) | 2 | Tension | Steady state | – | 17 | 20 °C, 500–1000 °C @100 °C | – | 5 °C/min | 0.5 mm/min |
| F | (c) | 2 | Compression | Steady state | – | 30 | 20–900 °C @100 °C | 50%, 80%, 100%, 120% of 0.2% proof stress (372,30 MPa) | 5 °C/min | 0.5 mm/min |
| G | (c) | 2 | Compression | Transient | – | 16 | – | | 5 °C/min<br>20 °C/min | – |
| H | (d) | 1 | Compression | – | – | 2 | Ambient | – | – | 0.5 mm/min |

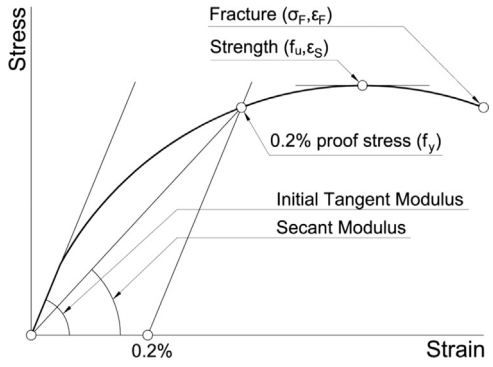


**Fig. 4.** Typical stress–strain diagram of cast iron in tension.

### 3.3. Ultimate strength in tension

The effect of temperature on the ultimate tensile strength, normalized to the ambient temperature value, is presented in Fig. 9a. The transient test strength values are higher than the steady state values and the transient tests conducted at 20 °C/min are slightly higher than those tested at 5 °C/min.

The strength reduction factor–temperature relationship of EN 1993-1-2 [36] for low carbon steel gives a safe low bound to the transient test results. The steady state test results give similar strength reduction factors as EN 1993-1-2 [36] for steel at temperatures higher than 400 °C. However, at lower temperatures up to 400 °C, there are some scatters in the test results with the average showing no effect of temperature, which is consistent with EN 1993-1-2 [36]. This indicates that at low temperatures, there is little effect of temperature on the strength of cast iron and the inconsistence most probably occurred because of the brittle nature of cast iron and the effects of flaws (which is determined by the number, size, orientation etc. of the flaws) on the strength of the material. For example, the ambient temperature strength values of the two duplicate test specimens (Group A) are 192 and 215 MPa.

In [24], the upper and lower bounds of the ultimate strength reduction factor were determined. They are shown in Fig. 9a and are consistent with the present test results if including both steady state and transient tests.

When a metal structure (cast iron or steel) is subject to fire attack, the structure temperature is likely to be higher than 400 °C. Also, since the heating condition is close to the transient testing condition, the transient testing results are more relevant. Therefore, a practical solution is to use the same EN 1993-1-2 [36] strength reduction factors for steel as for cast iron.

### 3.4. Yield stress

Fig. 9c shows yield stress (0.2% proof stress) reduction factor–temperature relationships. Also plotted in Fig. 9c are the lower and upper bounds suggested in [24], the EN 1993-1-2 curves for Young's modulus and yield strength of steel. The test results (including both steady-state and transient tests) are consistent with lower and upper bounds of [24]. The EN 1993-1-2 curve for Young's modulus of steel can be safely used to represent the 0.2% proof stress reduction factor–temperature relationship for cast iron. However, at temperatures exceeding 500 °C, in the EN1993-1-2 yield strength reduction factor–temperature relationship gives better approximation to the test results.

### 3.5. Young's modulus

Fig. 9b compares the secant modulus at 0.2% proof stress

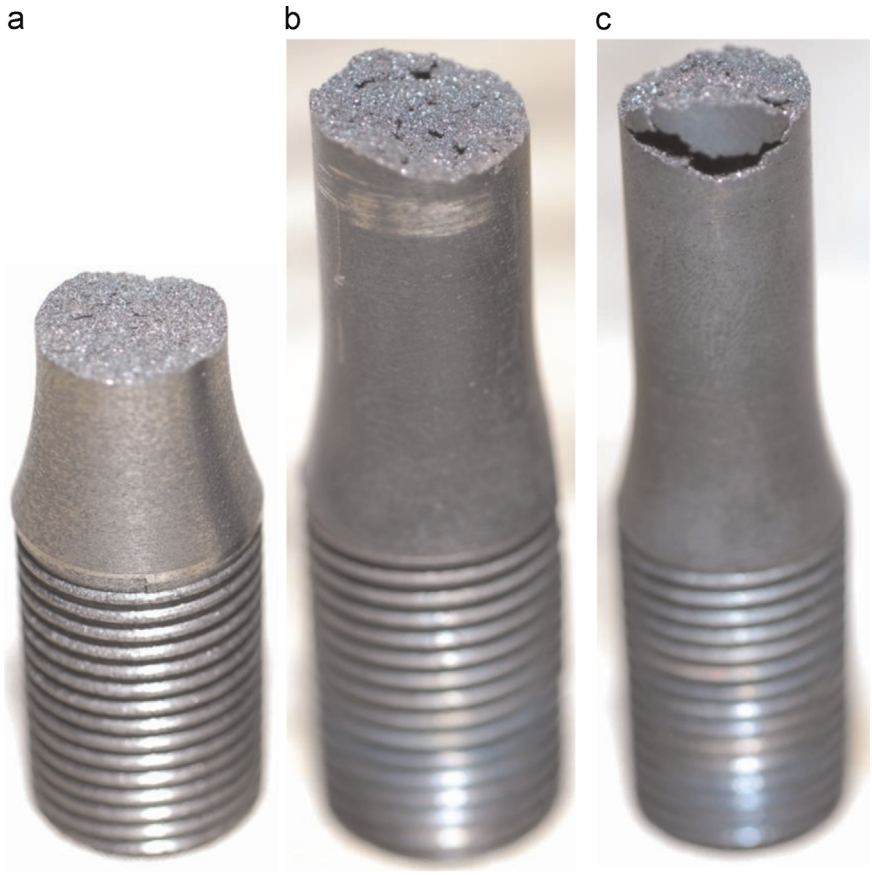


**Fig. 5.** Different intergranular fracture modes in tension: (a) brittle failure at room temperature, (b) moderately brittle fracture at 700 °C and (c) multi-surface moderately brittle fracture at 700 °C.

reduction factor–temperature relationship with EN 1993-1-2 relationship for Young's modulus of steel.

The secant modulus is calculated from the following relationship:

$$E = \sigma_{0.2\%}/\varepsilon_{0.2\%} \quad (1)$$

where $\sigma_{0.2\%}$ and $\varepsilon_{0.2\%}$ are the 0.2% proof stress and the corresponding strain respectively.

The results in Fig. 9b suggest that the EN 1993-1-2 [36] relationship for Young's modulus of steel is a safe lower bound approximation.

### 3.6. Elongation at the maximum stress (ultimate strength)

Fig. 9d presents elongations at the maximum stresses. There is large variation among the test results at the same temperature. However, a conservative value of $\varepsilon_u = 0.5\%$ may be considered. Alternative, the failure strain may be taken as unchanged at ambient temperatures.

### 3.7. Elongation at failure

At low temperatures (not exceeding 400 °C), the maximum elongation at failure is almost the same as the elongation at the maximum stress, indicating that cast iron has little ductility and fractures once it has reached its maximum stress. At high temperatures, cast iron becomes more ductile and fracture is delayed after reaching the maximum stress. Fig. 9e plots the maximum elongations. It shows that there is a good level of consistence among different tests results at the same temperature. The following equation (Eq. (2)) gives a close approximation to the test results:

$$\left.\begin{array}{l}\text{For} \quad 20\ ^\circ C \le \theta \le 400\ ^\circ C \\ \varepsilon_f = \varepsilon_{t,20} \\ \text{For} \quad 400\ ^\circ C < \theta \le 700\ ^\circ C \\ \varepsilon = \varepsilon_{t,20} + \varepsilon_{t,20}(\theta - 400\ ^\circ C)/100 \\ \text{For} \quad 700\ ^\circ C < \theta \le 900\ ^\circ C \\ \varepsilon = 4\varepsilon_{t,20} + 3\varepsilon_{t,20}(\theta - 700\ ^\circ C)/100\end{array}\right\} \quad (2)$$

The stress at fracture can be taken equal to the strength for temperatures up to 400 °C. For higher temperatures, this value can be taken as 50% of the strength although there is large scatter within the experimental data.

### 3.8. Proposed stress–strain relationship

For simplicity, a tri-linear (bilinear at temperatures not exceeding 400 °C) relationship may be used for the stress–strain relationship of cast iron at elevated temperatures. Fig. 10 shows this stress–strain curve and how the key points can be determined using the recommendations suggested in the previous sections.

## 4. Mechanical properties of cast iron in compression at elevated temperatures

### 4.1. General

The stress–strain diagram of cast iron in compression is totally

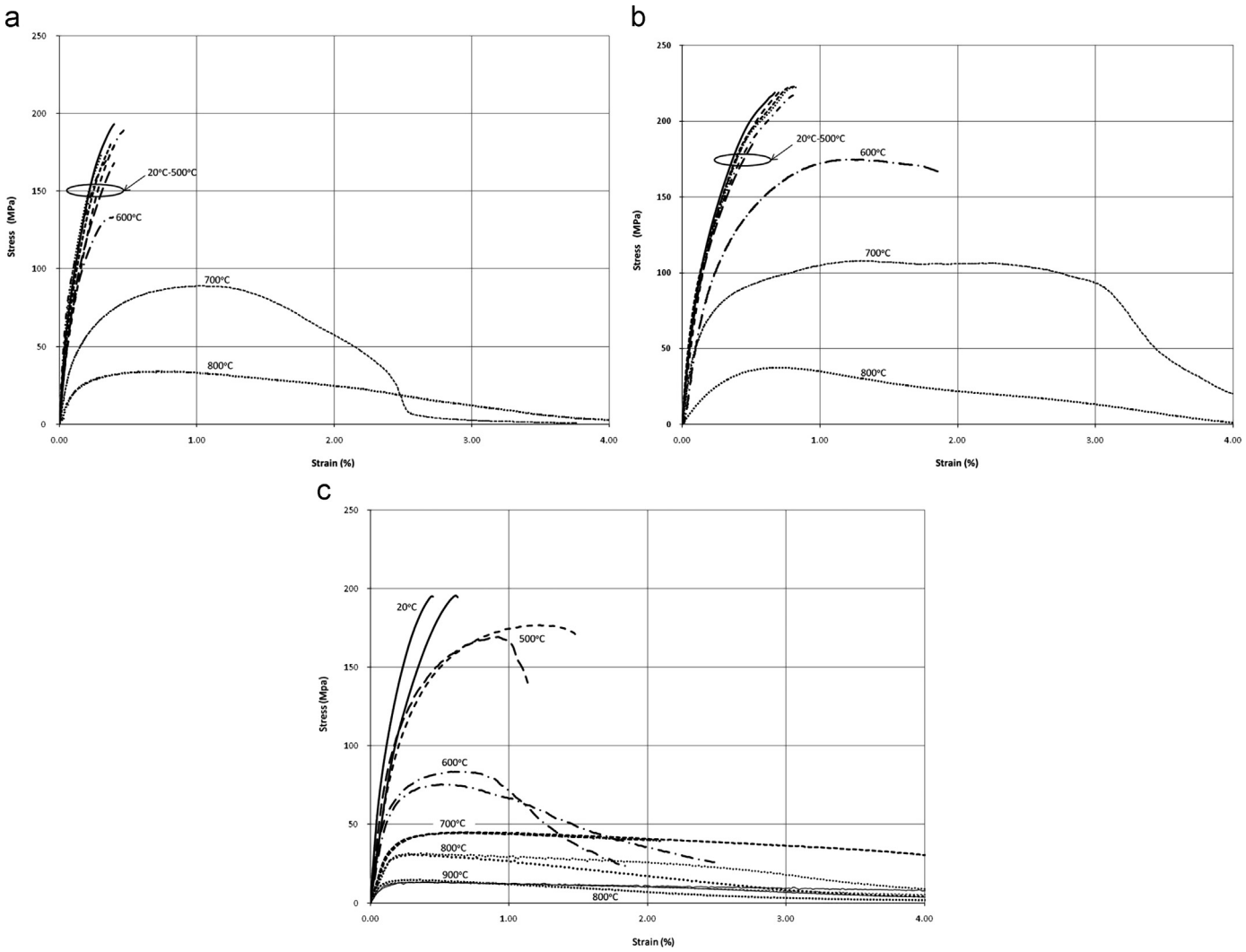


**Fig. 6.** Steady state results under tension: (a) and (b) Group A tests, (c) Group E tests.

different from that in tension. This happens because the flaws are closing in compression and they affect less the overall behavior (e.g. stiffness and strength) of cast iron.

Fig. 11 shows typical stress–strain diagram of cast iron in compression. Contrary to the tensile behavior, the modulus of elasticity and a proportional limit can be clearly defined. Conventionally, the yield strength is also assumed to be the 0.2% proof stress. Beyond the yield point, the material exhibits strain hardening which is defined by the hardening modulus $E_T$. Material failure is reached at the stress $f_u$. However, this point could not be accurately determined from all conducted experiments because the expansiometer had a limit of about 5% in compression at elevated temperatures. In order to gain some quantitative data on the strain limit of cast iron in compression, two additional tests at ambient temperatures were carried out. In these tests, thicker specimens (Fig. 1d) were used to reduce the influence of buckling. These specimens were prepared from the grip zones of the ambient temperature test specimens of Group A. Fig. 12a presents the stress–strain diagrams of these two experiments and Fig. 12b shows the failure mode. Shear failure occurred at approximately 10% compression strain. Because cast iron becomes more ductile at higher temperatures, the failure strain of cast iron in compression at elevated temperatures can be conservatively taken as 10%. The stress–strain curves show a relatively steep declining branch which resulted from the residual friction resistance of the failure surface.

Fig. 13a presents complete steady-state test results and Fig. 13b compares some of the steady-state test results with transient test results. During the transient tests, the stress in the test specimen increased due to restrained thermal expansion. This caused the strain to exceed 5% in many of the high temperature ( $>500$ °C) tests. As explained earlier, such data are unreliable. Therefore, the available data for the high temperatures is sporadic. Nevertheless, the comparison in Fig. 13b suggests that the steady-state and transient test results are reasonably close. Therefore, the properties of cast iron in compression are based on the steady-state test results.

### 4.2. Stress–strain curves in compression

Fig. 13a shows that at temperatures not exceeding 400 °C, there is little change in the stress–strain diagrams. At higher temperatures there is, as expected, a gradual decrease in the values of all the mechanical properties. Fig. 14 shows how the key parameters of the stress–strain diagram change at increasing temperatures. Plotted in Fig. 14 are also the relevant relationships for steel from EN 1993-1-2 [36].

### 4.3. Young's modulus

Fig. 14a shows reduction of Young's modulus with temperature.

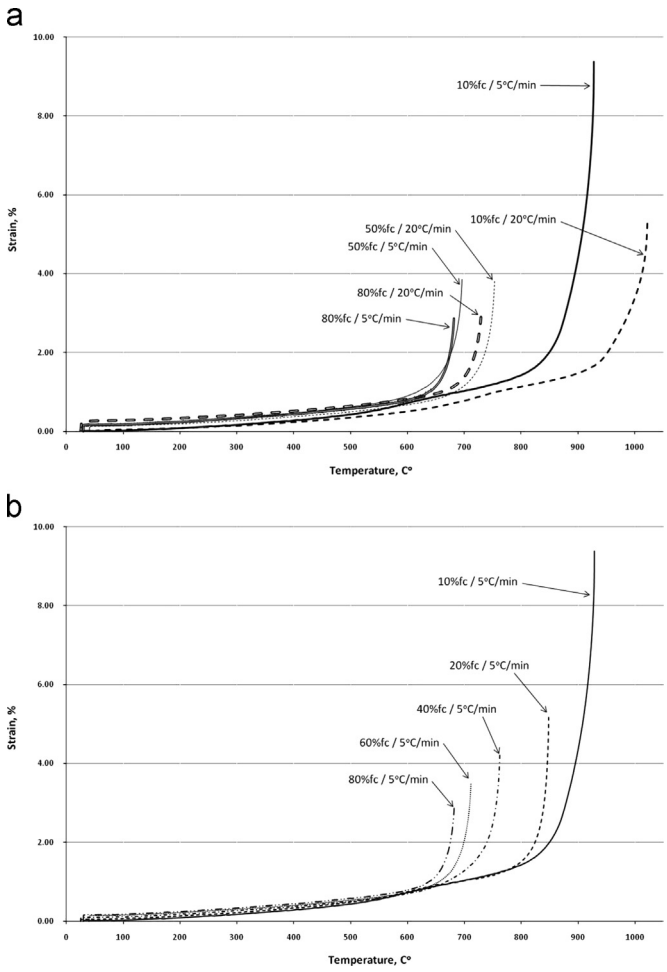


**Fig. 7.** The effect of (a) heating rate and (b) of utilization factor from Group B transient tests.

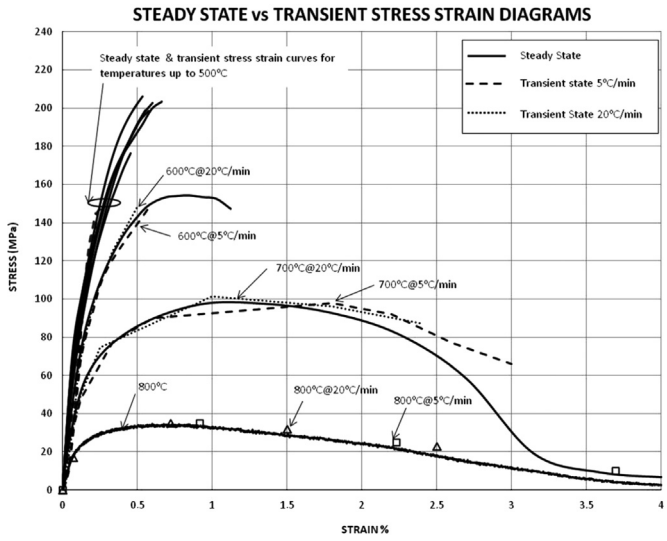


**Fig. 8.** Comparison of stress–strain curves from the steady-state and transient state tests.

Young's modulus in compression is obtained as the initial tangent modulus. Fig. 14a indicates that the EN 1993-1-2 Young's modulus–temperature relationship for steel is a close and safe approximation for cast iron in compression.

### 4.4. Proportional limit

In compression, cast iron exhibited a prolonged phase of approximately linear stress–strain behavior. The proportional limit of stress is approximately twice the yield stress (0.2% proof stress) in tension. Section 3.3 has suggested using the EN 1993-1-2 yield strength reduction factor–temperature relationship for steel. The results in Fig. 14b confirm this suggestion. In contrast, the EN 1993-1-2 proportional stress reduction factor–temperature relationship is too conservative.

### 4.5. Yield stress (0.2% proof stress)

Fig. 14c presents the reduction of yield stress with temperature. The steady state results are slightly lower than the transient test results. The transient test results are very similar to the EN 1993-1-2 results for steel. Therefore, the EN 1993-1-2 yield strength reduction factor–temperature relationship for steel can be used for cast iron in compression.

### 4.6. Ultimate strength in compression and strain hardening

The ultimate strength could not be determined from the elevated temperature experiments as explained in Section 3.3, except for that at ambient temperature. However, the analysis of results for cast iron in compression suggests that its relative behavior, between elevated and ambient temperatures, follow that of steel. Therefore, it is proposed that the reduction factors for ultimate strength of steel in tension in EN 1993-1-2 be used for cast iron in compression. The ultimate strength can then be used to determine the strain-hardening segment of the stress–strain curve in compression by limiting the strain at 10%, as shown in Fig. 12(a).

### 4.7. Stress–strain relationship in compression

Based on the discussions above, the stress–strain relationships of cast iron in compression (Fig. 15) can be constructed using a trilinear curve as described below:

(1) initial linear relationship until the proportional limit;
(2) linear relationship from the proportional limit until 0.2% proof stress; and
(3) final linear relationship from the 0.2% proof stress to the ultimate strength at 10% strain.

## 5. Coefficient of thermal expansion of structural cast iron

The coefficient of thermal expansion of cast iron was measured on three identical specimens of material 1 in Table 1, following the provisions of the American Standard ASTM E831-12 [37] with continuous monitoring of the specimen at increasing temperature. All the experiments were carried out using a 133459/TMA-7 Thermomechanical Analyzer (TMA). The initial temperature of the heating chamber was set at 10 °C and the heating rate was 10 °C/min.

The coefficient of thermal expansion was calculated using the following formula:

$$\alpha = (t_2 - t_1)/t_1^*(T_2 - T_1) \quad (3)$$

where (see Fig. 16) $\alpha$ is the coefficient of thermal expansion, in mm/mm °C, $t_1$ the thickness of specimen at point 1, in mm, $t_2$ the thickness of specimen at point 2, in mm, $t_2$ the thickness of specimen at point 2, in mm, $T_1$ the temperature at point 1, °K, $T_2$ the temperature at point 2, °K.

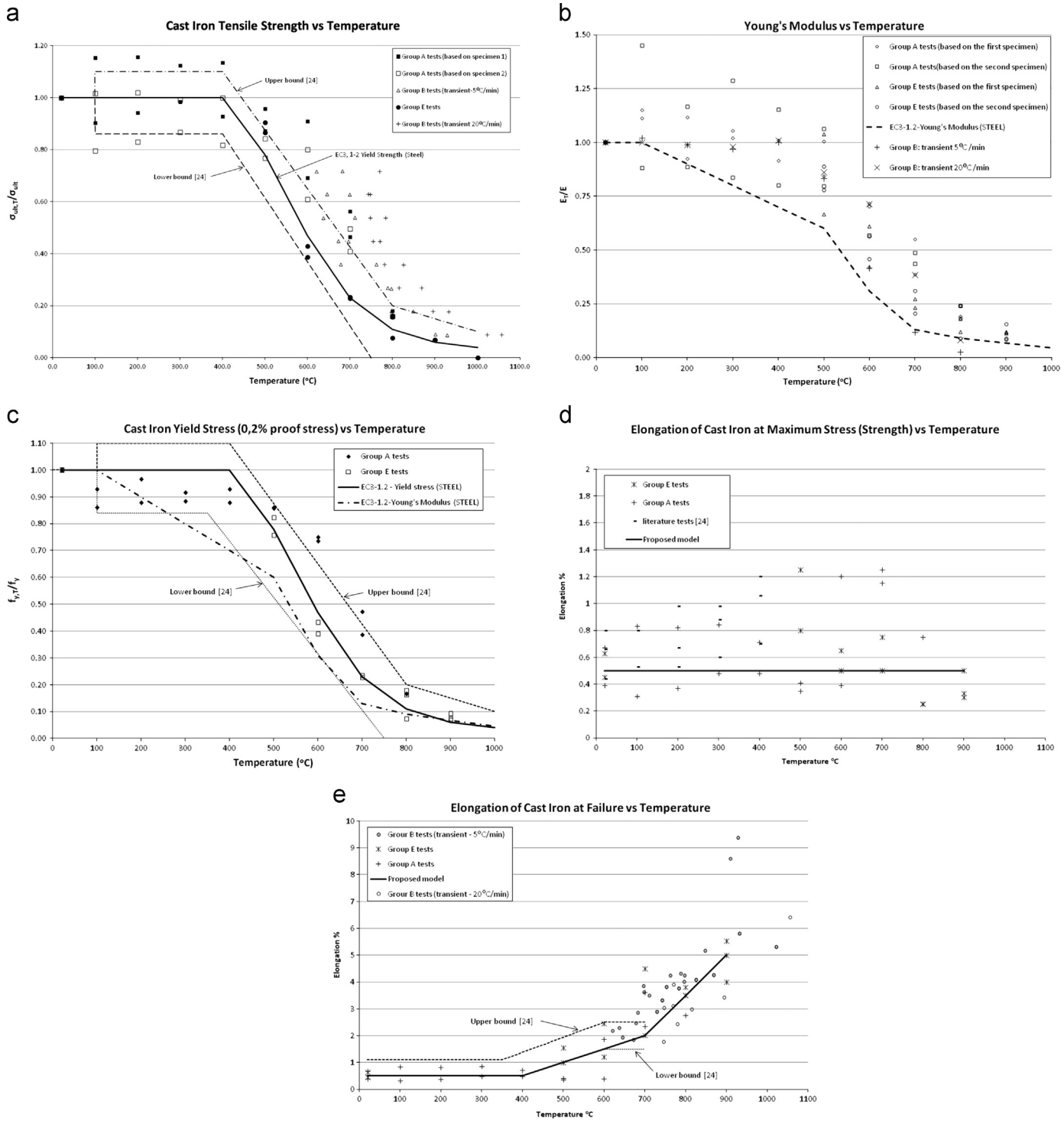


**Fig. 9.** Test results in tension for: (a) strength, (b) secant modulus at 0.2% proof stress, (c) 0.2% proof stress, (d) elongation at maximum stress (strength), and (e) elongation at failure.

In addition, a specimen with the shape shown in Fig. 1(c), made from material 2 (Table 1), was heated without imposing any load to measure its thermal strains.

Fig. 17(a) presents the coefficient of thermal expansion results for each specimen and also plots the average variation of the three test specimens. Also shown in Fig. 17(a) is the EN 1993-1-2 [33] relationship for steel. The experimental results follow the same trend of increasing coefficient of thermal expansion with increasing temperature as for steel. However, the test results for cast iron are lower than those of steel at low temperatures and higher than those of steel at high temperatures.

Fig. 17(b) compares the total thermal strain between the average test results and the EN 1993-1-2 values for steel. The two sets of results are close. Because it is the total thermal strain, not the coefficient of thermal strain, that will influence cast iron structural behavior in fire, it is proposed using the EN 1993-1-2 thermal strain

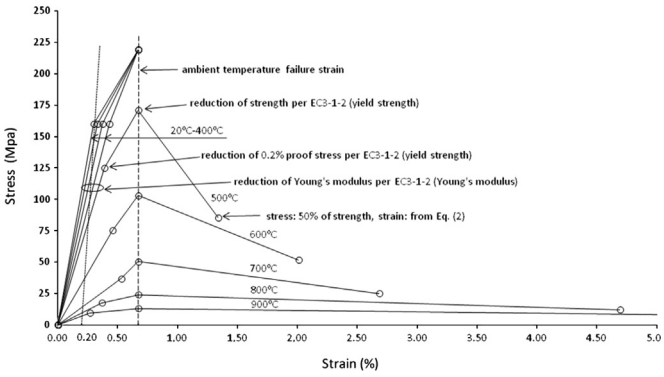


**Fig. 10.** Proposed stress strain temperature relationship of cast iron in tension.

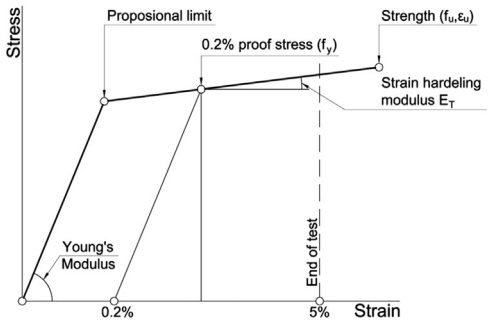


**Fig. 11.** Typical stress–strain diagram of cast iron in compression.

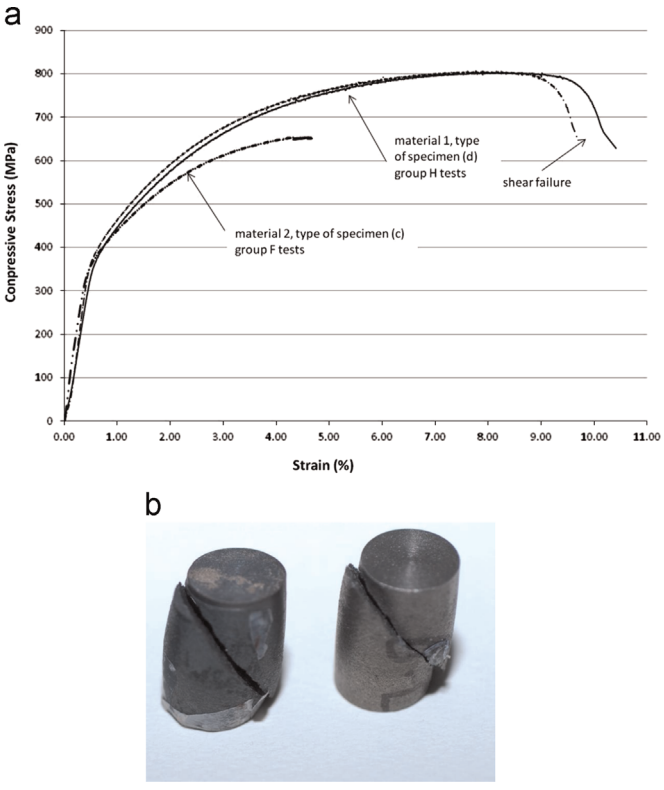


**Fig. 12.** (a) Ambient temperature stress–strain diagrams of cast iron (Group F and H tests) and (b) shear failure mode of Group H specimens.

values of steel for cast iron. The test results for cast iron do not show phase change effect around 750 °C. However, since this temperature is very high and likely to be outside the range of practical interest, it is suggested not necessary to refine the results for cast iron.

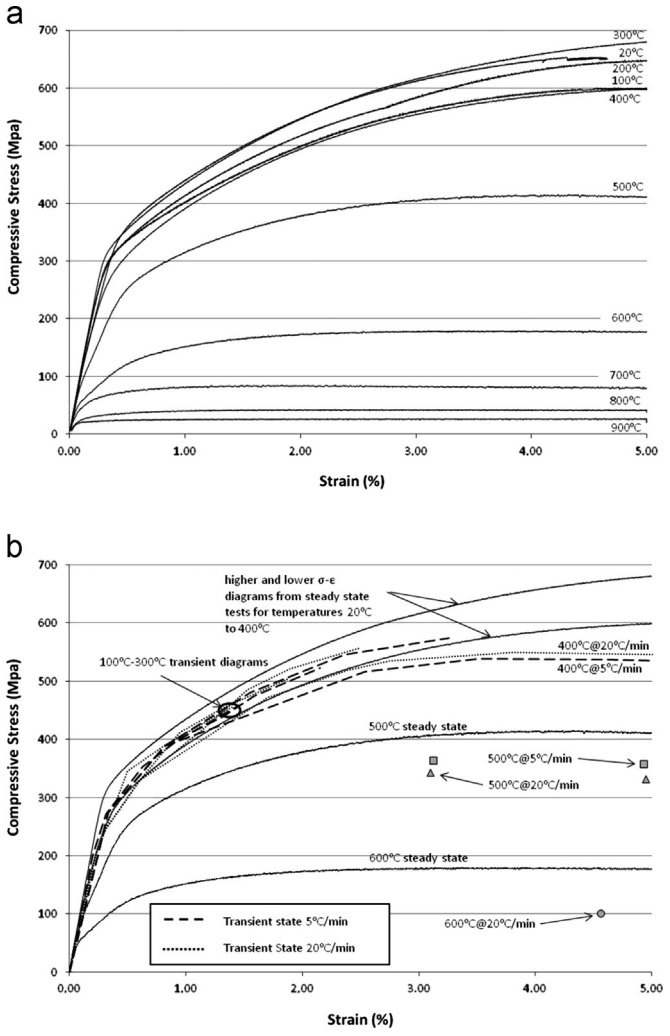


**Fig. 13.** (a) Steady state stress–strain curves and (b) comparison of steady-state and transient test stress–strain curves in compression.

## 6. Residual strength of structural cast iron

Cast iron structures are historic structures and are often preserved whenever possible, even after fire damage. To assess whether a cast iron structure is reparable after fire damage, it is necessary to obtain mechanical properties of cast iron after cooling down. In particular, cast iron has been described as a material susceptible to thermal shock during fire-fighting [38]. So far, there is a complete lack of data in open literature.

In this research, two cooling method types (rapid cooling by water quenching and slow cooling in ambient air) were used for the Group D test specimens in Table 2. Fig. 18 shows the heating and cooling histories of the specimens, for specimens being heated to 800 °C and then cooled. Fig. 19 shows the experimental residual strength results and compares them with experimental results for other types of steel [39,40]. These suggest that the cooling rate has some influence on the residual strength of cast iron. The test results show that the residual strength of cast iron remains practically unchanged up to 500 °C, then undergoes the maximum reduction (approximately 20% for slow cooling and 40% for rapid cooling) in the temperature region of 600–700 °C and then increases up to the ambient temperature value at 800 °C.

This is to be expected, because the heating and cooling process is a hardening procedure for metals [41]. According to Digges et al. [41], austenite decomposes at temperatures around 720 °C. Depending on the cooling rate, Austenite may recompose (very slow

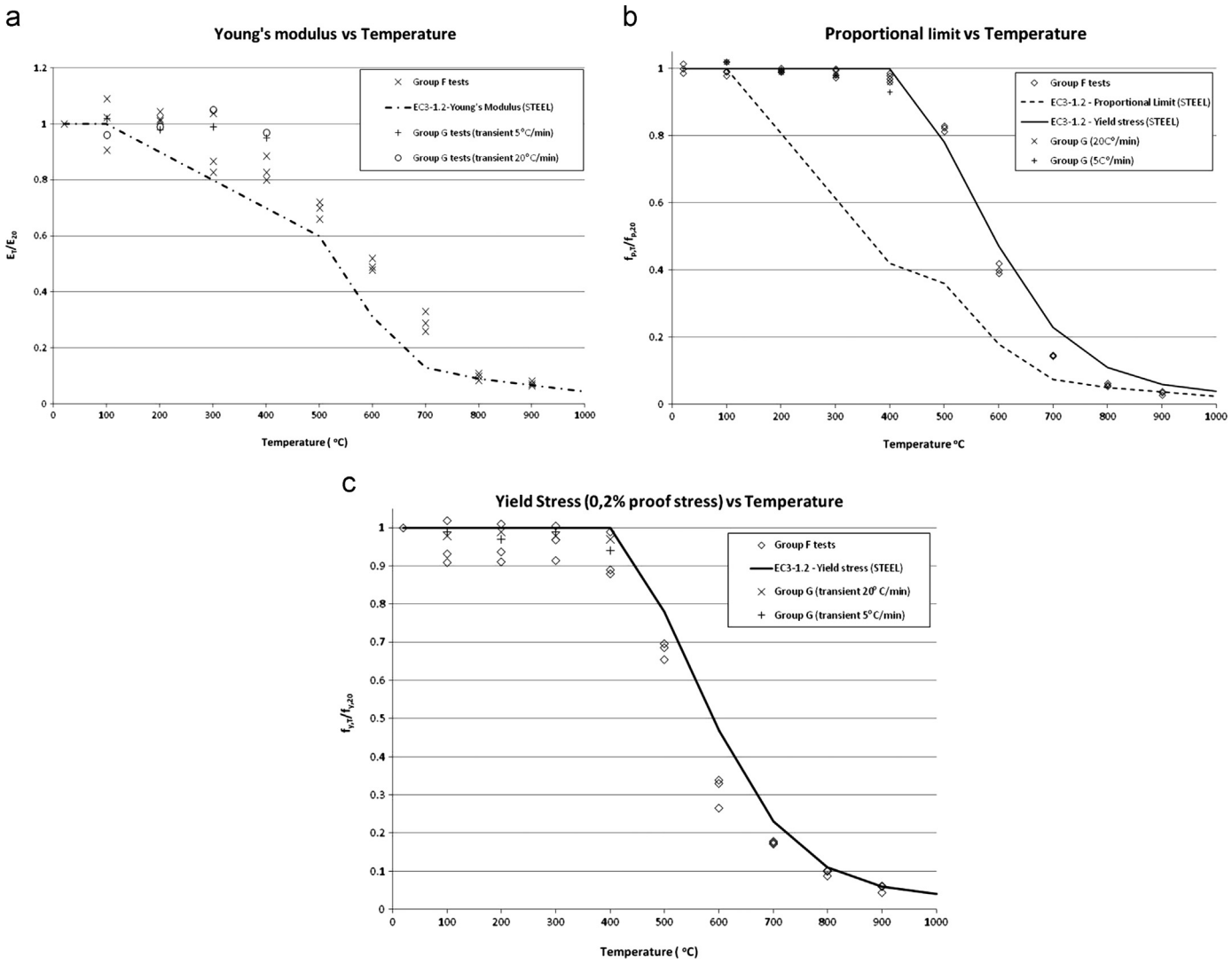


**Fig. 14.** Reduction factor–temperature relationships for cast iron in compression: (a) Young's modulus; (b) proportional limit; and (c) yield strength.

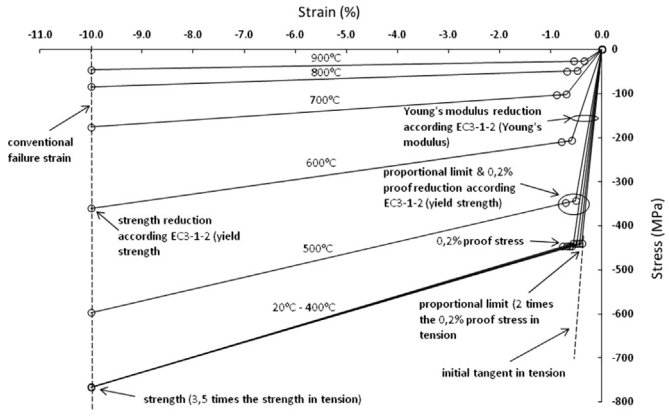


**Fig. 15.** Proposed stress–strain relationships of cast iron in compression.

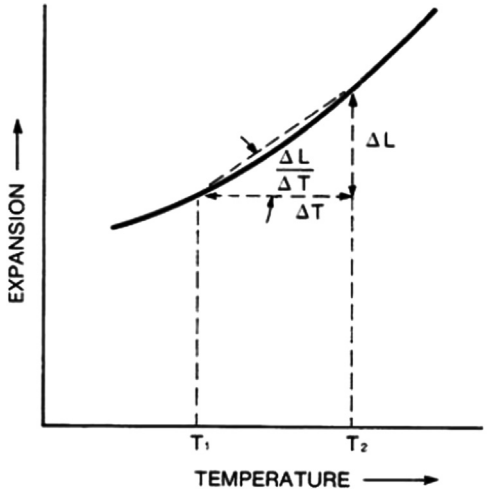


**Fig. 16.** Calculation of thermal expansion [37].

cooling rate-equilibrium conditions) or convert to pearlite or/and martensite (high cooling rates). The transformation of Austenite to pearlite/martensite increases the strength and hardness of the metal. Cast iron is not different [41] in behavior from eutectoid carbon steel, because a major portion of the carbon content is encountered in graphite flake form. Fig. 20 illustrates the influence of cooling rate and the relevant transformations.

Cast iron structures were historically designed with very high safety factors (ranging from 3 to 12 according to [9,23,22,43]). Therefore, this research suggests that despite the scatter in their mechanical properties, the reinstatement/reuse of cast iron

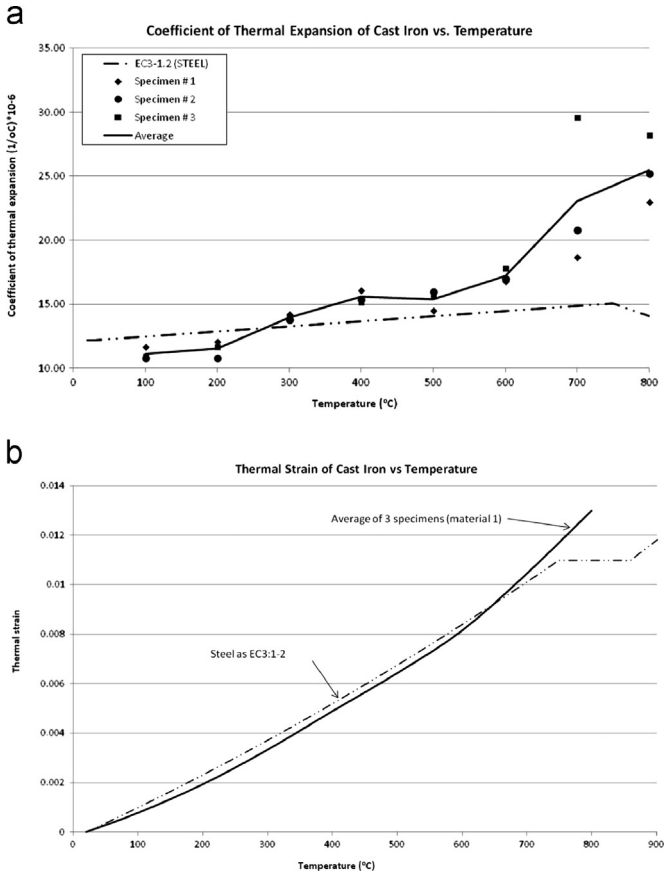


**Fig. 17.** Comparison of (a) thermal expansion variation with temperature and (b) thermal strain variation with temperature.

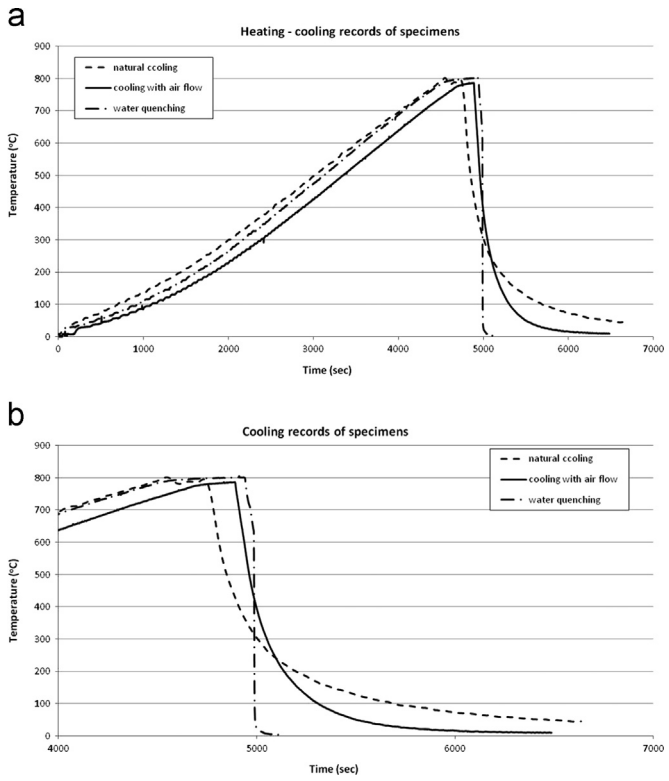


**Fig. 18.** Heating and cooling histories: (a) entire history and (b) enlarged view.

structures after fire attack, in most cases, is feasible if no visible damage or distortion can be detected.

## 7. Conclusions

This paper has presented the results of an extensive set of mechanical test results for cast iron at ambient and elevated temperatures, including tensile and compressive tests, under both steady-state and transient heating conditions, and cooling from high temperatures. Based on analysis of the test results, the mechanical properties of cast iron at elevated temperatures can be determined as follows:

### *7.1. Tensile stress–strain relationship*

The proposed tensile stress strain relationship is bilinear up to 400 °C and trilinear for higher temperatures. To derive the stress–strain temperature relationship, the following procedure should be applied:

- Determination of the bilinear stress–strain relationship at ambient temperature. This should include the initial linear part until the 0.2% proof stress and the second part from the 0.2% proof stress to the ultimate strength/fracture strain.
- At elevated temperatures, Young's modulus should be reduced according to the EN 1993-1-2 relationship for Young's modulus of steel.
- The 0.2% proof stress should be reduced according to the EN 1993-1-2 relationship for the yield strength of steel.
- The ultimate strength should be reduced according to the EN 1993-1-2 relationship for the yield strength of steel. The fracture strain at the ultimate strength should be the same as the failure strain at ambient temperature.
- For temperatures higher that 400 °C, a descending line from the ultimate strength point should be introduced. The stress at the final point is 50% of the ultimate strength and the final fracture strain is obtained from Eq. (2).

### *7.2. Compressive stress–strain relationship*

- The proposed compressive stress strain relationship is trilinear. The initial linear relationship until the proportional limit, the second linear part from the proportional limit to the 0.2% proof stress and then the final line from the 0.2% proof to the ultimate strength at 10% strain.
- The proportional limit, the 0.2% proof stress and the ultimate strength should be reduced based on the ambient temperature values according the EN 1993-1-2 relationship for the yield strength of steel. The strain at the ultimate strength can be conservatively taken as 10% for all temperatures.
- Young's modulus should be reduced according the EN 1993-1-2 relationship for Young's modulus reduction of steel.

### *7.3. Coefficient of thermal expansion*

The thermal strain–temperature relationship of cast iron can be assumed to be the same as that of steel in EN 1993-1-2.

### *7.4. Residual strength after cooling*

The limited number of tests of this paper suggests that after cooling to ambient temperature, cast iron regains its strength as structural steel. Its strength is fully recovered at temperatures

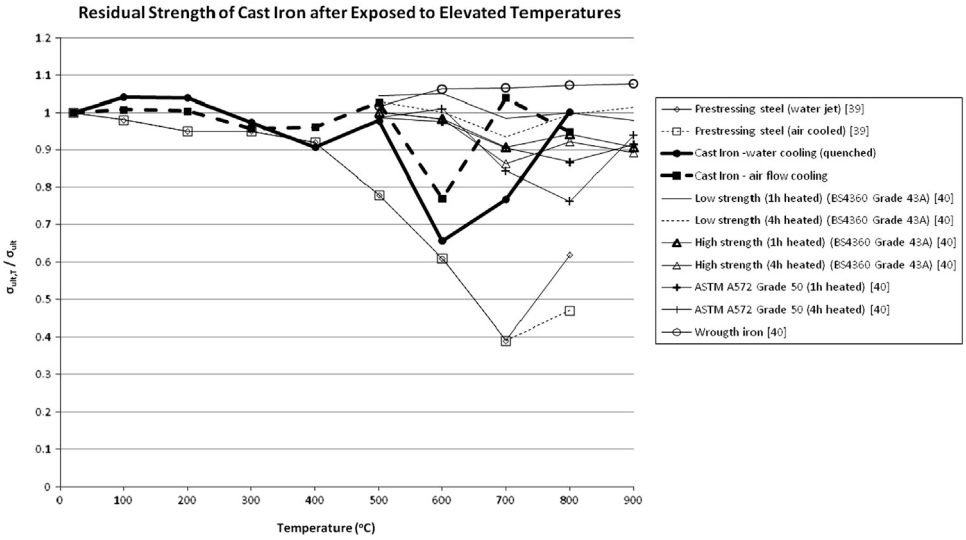


**Fig. 19.** Comparison of residual strength of cast iron after exposure to elevated temperatures with those of wrought iron and structural and prestressing steels.

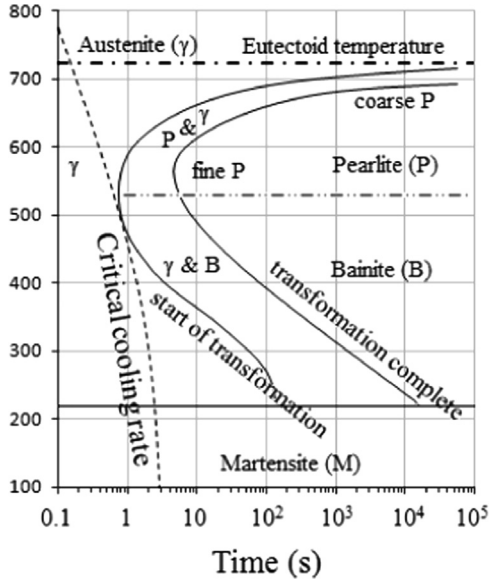


**Fig. 20.** Schematic diagram illustrating isothermal curves (IT), critical cooling curves and resulting microstructures for eutectoid steel [42].

below 600 °C and higher than 700 °C. Between these temperatures, the maximum loss of strength is about 20–40%, depending on the cooling method. Taking into account the large safety factors used in design of historic cast iron structures, the results of this research suggest that cast iron structures can be restored after fire damage provided there is no visible damage.

## References


[1] Institution of Structural Engineers, Appraisal of Existing Structures, second edition, The Institution of Structural Engineers, London, UK., 1996.
[2] T. Bonson, The first iron-framed building? Ind. Archaeol. Rev. XXII (1) (2000) 63–66.
[3] K.A. Falconer, Fireproof mills – the widening perspectives, Ind. Archaeol. Rev. XVI (1) (1993) 11–26.
[4] R. Fitzgerald, The development of the cast iron frame in textile mills to 1850, Ind. Archaeol. Rev. X (2) (1998) 127–145.
[5] D. Friedman, Historical Building Construction, Norton & Company Publishers, New York, USA, 1995.
[6] P. Gerber, The flax spinning mill in Myslakowice near Jelenia Gora, PolandInd. Archaeol. Rev. XIII (2) (1991)142–151.
[7] S.B. Hamilton, Old cast-iron structures, Struct. Eng. 4 (1949) 173–191.
[8] I. Wouters, M. Bouw, The development of fireproof construction in Brussels between 1840–1870, Ind. Archaeol. Rev. XXVIII (1) (2006) 17–31.
[9] T. Swailes, 19th Century fireproof' buildings, their strength and robustness, Struct. Eng. 81 (19) (2003) 27–34.
[10] T.M.D. Silva, D.G. Church, Strengthening two London underground covered ways, Proc. Inst. Civ. Eng. Transp. 158 (TR3) (2005) 139–147.
[11] D. Friedman, Cast-iron-column strength in renovation design, J. Perform. Constr. Facil. 9 (3) (1995) 220–230.
[12] M. Parmenter, An investigation of the strength of cast iron beams (Ph.D. thesis), Department of Civil and Structural Engineering, UMIST, UK, 1996.
[13] J. Rondal, K.J.R. Rasmussen, On the strength of cast iron columns, J. Constr. Steel Res. (2003)1257–1270.
[14] I. Brooks, A. Browne, D.A. Gration, A. McNulty, Refurbishment of St Pancras – justification of cast iron columns, Struct. Eng. 3 (2008) 28–39.
[15] J.R. Barnfield, A.M. Porter, Historic buildings and fire: fire performance of cast-iron structural elements, Struct. Eng. 62A (12) (1984) 373–380.
[16] A. Baxter, New concordia wharf, fire engineering aspects, Archit. J. 180 (27) (1984) 58.
[17] A. Porter, The behavior of structural cast iron in fire, Engl. Herit. Res. Trans. 1 (1998) 11–20.
[18] I. Wouters, M. Mollaert, Evaluation of the fire resistance of 19th century iron framed buildings, Fire. Technol. 38 (2002) 383–390.
[19] G.G. Nieuwmeijer, Fire resistance of historic iron structures in multistory buildings, Trans. Built Environ. 55 (2001) 39–48.
[20] F. Wald, M. Dagefa, Fire Resistance of Cast Iron Columns in Vinohrady Brevery, Application of Structural Fire EngineeringPrague, Czech Republic (2011) 443–448.
[21] I.L. Twilt, Fire Resistance of Cast Iron Structures in Historic Buildings, Urban Heritage Building Maintenance, Iron & Stee, The Netherlands (1999) 99–106.
[22] D. Dibb-Fuller, R. Fewtrell, R. Swift, Windsor Castle: fire behaviour and restoration aspects of historic ironwork, Struct. Eng., 76, 367–372.
[23] M.N. Bussell, M.J. Robinson, Investigation, appraisal, and reuse, of a cast-iron structural frame, Struct. Eng. 76 (3) (1998) 37–42.
[24] C. Maraveas, Y.C. Wang, T. Swailes, Thermal and mechanical properties of 19th century fireproof flooring systems at elevated temperatures, Constr. Build. Mater. 48 (2013) 248–264.
[25] J.R. Kattus, B. McPerson, Report on Properties of Cast Iron at Elevated Temperatures, ASTM Special Technical Publication No. 248, Philadelphia, USA, 1959.
[26] K.B. Palmer, High Temperature Properties of Cast Irons, Conference on Engineering Performance of Iron Castings, British Cast Iron Research Association (1970) 217–249.
[27] J.W. Donaldson, Low-temperature heat treatment of special cast irons, Foundry Trade J. 31 (1925) 517–522.
[28] T.H. Angus, Cast Iron: Physical and Engineering Properties, 2nd ed., Butterworths, London–Boston, 1976.
[29] C. Maraveas, Y.C. Wang, T. Swailes, Fire resistance of 19th century fireproof flooring systems: a sensitivity analysis, Constr. Build. Mater. 55 (2014) 69–81.
[30] ISO 6892-1:2009, Metallic Materials – Tensile testing – Part 1: Method of test at Room Temperature, International Organization for Standardization, Switzerland, 2009.
[31] ASTM E9-09, Standard Test Methods of Compression Testing of Metallic Materials at Room Temperature, American Society for Testing and Materials, USA, 2009.
[32] ASTM E209-00, Standard Practice for Compression Tests of Metallic Materials at Elevated Temperatures with Conventional or Rapid Heating Rates and Strain Rates, American Society for Testing and Materials, USA, 2010.

[33] G.N.J. Gilbert, An evaluation of the stress/strain properties of flake graphite cast iron in tension and compression, Research Report No. 514, BCIRA J. Res. Dev. 7 (1959) 745–789.
[34] T. Swailes, 19th Century cast-iron beams: their design, manufacture and reliability, Proc. Inst. Civ. Eng. Civ. Eng. 114 (1995) 25–35.
[35] B.R. Kirby, R.R. Preston, High temperature properties of hot-rolled, structural steels for use in fire engineering design studies, , Fire Saf. (13, 1988) 27–37.
[36] European Standard EN 1993-1-2, . Eurocode 3-Design of steel structures—Part 1-2: General Rules—Structural Fire Design, European Committee for Standardization, Brussels, Belgium, 2005.
[37] ASTM E831-12, Standard Test Method for Linear Thermal Expansion of Solid Materials by Thermomechanical Analysis, American Society for Testing and Materials, USA, 2012.
[38] F.L. Brannigan, Cast iron and steel, Fire Eng. 159 (2006) 126.
[39] I. Cabrita Neves, Joao Paulo C. RodriguesAntonio de Padua Loureiro, , Mechanical properties of reinforcing and prestressing steels after heating, J. Mater. Civ. Eng. 8 (1996) 189–194.
[40] C.I. Smith, B.R. Kirby, D.G. Lapwood, K.J. Cole, A.P. Cunningham, R.R. Preston, The reinstatement of fire damaged steel framed structures, Fire Saf. J. 4 (1981) 21–62.
[41] T.G. Digges, S.J. Rosenberg, G.W. Geil, Heat Treatment and Properties of Iron and Steel, Monograph 88, National Bureau of Standards, Department of Commerce, USA, 1966.
[42] G.F. Vander Voort, Atlas of Time–Temperature Diagrams for Irons and Steels (Materials Data Series), Materials Park, Ohio, 1991.
[43] T. Swailes, Scottish Iron Structures, Guide for Practitioners, UK, Historic Scotland, Edinburgh, 2006.